MOLECULAR AND CELLULAR BIOLOGY, Oct. 2011, p. 4144–4154 Vol. 31, No. 19
0270-7306/11/$12.00 doi:10.1128/MCB.05532-11

Klf1 Affects DNase II-Alpha Expression in the Central Macrophage of a Fetal Liver Erythroblastic Island: a Non-Cell-Autonomous Role in Definitive Erythropoiesis▽

Susanna Porcu,[1] Maria F. Manchinu,[1] Maria F. Marongiu,[1] Valeria Sogos,[2] Daniela Poddie,[1] Isadora Asunis,[1] Loredana Porcu,[3] Maria G. Marini,[1] Paolo Moi,[3] Antonio Cao,[1,3] Frank Grosveld,[4] and Maria S. Ristaldi[1]*

Istituto di Ricerca Genetica e Biomedica, Consiglio Nazionale delle Ricerche, Cagliari, Sardinia, Italy[1]; Dipartimento di Citomorfologia, Facoltà di Medicina, Università di Cagliari, Cagliari, Sardinia, Italy[2]; Dipartimento di Scienze Biomediche e Biotecnologie, Facoltà di Medicina, Università di Cagliari, Cagliari, Sardinia, Italy[3]; and Department of Cell Biology, Erasmus University, Rotterdam, Netherlands[4]

Received 21 April 2011/Returned for modification 1 June 2011/Accepted 24 July 2011

A key regulatory gene in definitive erythropoiesis is the erythroid Kruppel-like factor (*Eklf* or *Klf1*). *Klf1* knockout (KO) mice die *in utero* due to severe anemia, while residual circulating red blood cells retain their nuclei. *Dnase2a* is another critical gene in definitive erythropoiesis. *Dnase2a* KO mice are also affected by severe anemia and die *in utero*. DNase II-alpha is expressed in the central macrophage of erythroblastic islands (CMEIs) of murine fetal liver. Its main role is to digest the DNA of the extruded nuclei of red blood cells during maturation. Circulating erythrocytes retain their nuclei in *Dnase2a* KO mice. Here, we show that Klf1 is expressed in CMEIs and that it binds and activates the promoter of *Dnase2a*. We further show that *Dnase2a* is severely downregulated in the *Klf1* KO fetal liver. We propose that this downregulation of *Dnase2a* in the CMEI contributes to the *Klf1* KO phenotype by a non-cell-autonomous mechanism.

Erythroid Kruppel-like factor (Eklf/Klf1) (for a review, see Bieker [1]) is the founding member of the mammalian Kruppel-like family (Klf) of zinc finger transcription factors (for a review, see the work of Pearson et al. [31]). It was first isolated by subtractive hybridization with the intent to identify erythroid-specific transcription factors (25). Its expression was first thought to be restricted to erythroid and mast cells (25, 44). However, Klf1 expression has also been previously reported in primary macrophages (23).

Klf1 strongly binds to the CCACACCC sequence of the adult human β-*globin* gene, and it has been shown to activate the β-*globin* gene promoter (19, 25). Mutations of the CACCC box of the β-*globin* gene cause β-thalassemia in humans, which correlates to the lack of Klf1 binding to the promoter (9). Klf1 is also important in the γ-to-β-globin switching (4, 32, 38, 51, 52), for the function of the β-globin locus control region (LCR) (13), and for the active spatial organization of the β-globin locus (5), and it is critical in the formation of nuclear erythroid transcription factories (40).

Klf1 knockout (KO) mice are strongly anemic and die at around embryonic day 15 (E15), with a marked decrease in β-*globin* gene expression compared to that of the wild-type (wt) littermates, and circulating red blood cells retain the nuclei (29, 33, 34). Subsequent observations revealed that the *Klf1* KO phenotype is far more complex and impairs definitive erythropoiesis by molecular mechanisms in addition to the α/β-globin imbalance (β-thalassemia) (6, 14, 28, 36). Two observations are of particular interest. (i) The phenotype of the *Klf1* KO is far more severe than that of the murine β-thalassemia major model in which both β-major and β-minor globin genes are deleted (3). (ii) The null phenotype could not be rescued by γ-globin expression *in vivo*, despite the correction of the globin imbalance (and therefore of β-thalassemia) (33).

Studies based on the expression profiling by microarray and subtractive hybridization have shown that additional genes are downregulated in *Klf1* KO erythroid cells (6, 14, 28, 36). The additional target genes include AHSP (14, 36), dematin (band 4.9 protein) (6) and other erythrocyte membrane and cytoskeleton proteins (28), heme synthesis enzymes (14), transcription factors (12, 52), blood group antigens (14, 28), and genes involved in cell cycle regulation (35, 42, 45, 46). These studies suggest that the *Klf1*-null phenotype was exacerbated by the downregulation of these additional genes. However, taken together, these data still do not fully explain the lethal impaired definitive erythropoiesis of the *Klf1* KO phenotype. In *Klf1*-null mice, primitive embryonic erythropoiesis allows the embryos to survive until fetal liver definitive erythropoiesis takes place (29, 34), even though most of the genes affected by *Klf1* deprivation are expressed in the embryonic and definitive erythroid cells (6, 14, 28, 36). This observation suggests that other genes involved in definitive erythropoiesis may be involved, in addition to those already identified. Recent evidence suggests that the number of Klf1 binding sites has been underestimated (47). Some ameliorating effects have been reported by the expression of human γ-globin in *Klf1* KO/wt chimeric mice (20). These mice contained mature definitive enucleated erythrocytes of $Klf1^{-/-}$ origin (20). This comparison between the data obtained using chimeras and those obtained with the full *Klf1*

* Corresponding author. Mailing address: Istituto di Ricerca Genetica e Biomedica del Consiglio Nazionale delle Ricerche, Cittadella Universitaria di Cagliari, S.S. 554 bivio per Sestu, 09042 Monserrato (CA), Italy. Phone: 390706754592. Fax: 390706754652. E-mail: ristaldi@inn.cnr.it.

▽ Published ahead of print on 1 August 2011.

KO mice suggests that there may be a contribution of a non-cell-autonomous mechanism to the phenotype of *Klf1* KO mice. A possible non-cell-autonomous role of Klf1 has been previously suggested (33), but all of the genes described to date that are involved in the *Klf1* KO phenotype are cell autonomous (6, 12, 14, 28, 29, 34, 35, 36, 42, 45, 52). One possible candidate is *Dnase2a* (for a review, see the work of Evans and Aguilera [7]). DNase II-alpha is known to be involved in definitive erythropoiesis, and it is expressed in the central macrophage of erythroblastic islands (CMEI), where it is involved in the digestion of extruded nuclei of developing erythrocytes (for a review, see the work of Nagata [27]). *Dnase2a* is located 3.9 kb downstream of the *Klf1* gene in the mouse genome. The *Dnase2a* KO has a peculiar erythroid phenotype. The mice die around E17 of lethal anemia, which is thought to be caused by β-interferon (IFN-β) production by macrophages (49). IFN-β produced in the fetal liver inhibits erythropoiesis that occurs in association with macrophages at the erythroblastic island. Undigested DNA directly stimulates CMEIs to express IFN-β and, therefore, interferon-responsive genes, which inhibit erythropoiesis and kill the embryos. Klf1 and globins are expressed normally in *Dnase2a*-null mice (49).

Interestingly, *Dnase2a*$^{-/-}$ embryos display characteristic definitive circulating erythrocytes that retain their nucleus (16). *Klf1* and *Dnase2a* KO phenotypes present some similarities, such as ineffective definitive erythropoiesis and the presence of circulating nucleated definitive red blood cells (16, 29, 34, 49).

Here, we have aimed to determine whether *Dnase2a* is Klf1 dependent, because this would explain some of the unexplained phenotypic results of the *Klf1* KO. We evaluated the DNase II-alpha expression level in *Klf1* KO fetal liver, which revealed a dramatic reduction of *Dnase2a* mRNA and enzymatic activity. In addition, interferon-β is activated and a reduced number of central macrophages with abnormal shape are present in the *Klf1* KO fetal liver. Klf1 is expressed in CMEI nuclei and binds and activates the *Dnase2a* promoter. Analysis of isolated macrophages from wt fetal liver confirmed the expression of Klf1 and established the occupancy of the *Dnase2a* promoter by Klf1 *in vivo*. *Dnase2a* is strongly upregulated in CMEIs. Downregulation of *Klf1* by lentivirus-mediated RNA interference correlates with decreased expression of *Dnase2a* in primary CMEIs.

We propose that the downregulation of *Dnase2a* in the CMEI contributes to the impairment of definitive erythropoiesis through IFN-β production, which is the first indication of the involvement of Klf1 in a non-cell-autonomous biological mechanism.

MATERIALS AND METHODS

Genotyping. The original *Klf1* knockout (KO) mouse (29) line was maintained on a hybrid C57BL/6/CBA/J background. Genotypes were determined by PCR from genomic DNA using a pair of primers in the neomycin-resistant gene (*Neo*/Fw, 5′-ATGGGATCGGCCATTGAAC-3′; *Neo*/Rv, 5′-CTCGTCCTGCAGTTCATTC-3′) and a pair of primers in the *Klf1* gene (*Klf1*/Fw, 5′-CCACACACATATCGCACAC-3′; *Klf1*/Rv, 5′-TGCCGCCTCCCACACACACTC-3′) to discriminate between the wild-type and mutant alleles of the *Klf1* gene.

RNA analysis. Total RNA was extracted both from fetal liver and from fetal liver-isolated macrophage cells of E13.5 and E14.5 *Klf1*$^{+/+}$, *Klf1*$^{+/-}$, and *Klf1*$^{-/-}$ mice using TRIzol reagent (Life Technologies, Inc.), as described by the manufacturer's protocol. The cDNA was made from total RNA using Superscript II reverse transcriptase (Invitrogen) according to the manufacturer's recommendations. Semiquantitative reverse transcription-PCRs (RT-PCRs) were carried out using 220 bp DNase II-alpha cDNA generated by performing PCR with specific primers for the mouse *Dnase2a* gene together with mouse β-*actin* primers used as an internal control. The primers sequences were as follows: Exon2 m*Dnase2a*/Fw, 5′-GCAGCCATTGTACCGAAAG-3′; Exon5 m*Dnase2a*/Rv, 5′-AGGTTTGAGCATTAGGAGG-3′; mouse β-*actin*/Fw, 5′-CAGGCACCAGGGCGTGATGGT-3′; and mouse β-*actin*/Rv, 5′-CTCAACATGATCTGGGTCATC-3′. Reactions were carried out in the Gene Amp PCR system 9600. The conditions were chosen so that none of the cDNAs analyzed reached a plateau at the end of the amplification protocol. Aliquots of the PCR products at 28, 30, and 32 cycles were run on a 5% acrylamide gel, and the band intensity was analyzed by ethidium bromide staining. Some experiments were performed using both the m*Dnase2a* and the β-*actin* reverse primers end-labeled with [γ-^{32}P]ATP.

Northern hybridization assay. Up to 6 μg of total RNA from the E14.5 fetal liver of *Klf1*$^{+/+}$ and *Klf1*$^{-/-}$ mice was separated on a 1.5% agarose gel containing 2% (wt/vol) formaldehyde, transferred to a Hybond N^{+} membrane (Amersham Biosciences), and hybridized under low-stringency conditions (42°C) using mouse *Dnase2a* cDNA (pCMVsport 6.1-MGC clone ID 5397016), mouse *Klf1* cDNA (pT7T3D-PacI-RZPD clone ID IMAG p998G061136Q1), and mouse β-*actin* cDNA (220-bp PCR fragment) as probes.

Real-time quantitative PCR (RT-qPCR). RT-qPCRs were performed with the Applied Biosystems TaqMan kit as described by the manufacturer by using an ABI PRISM 7700 thermocycler (Applied Biosystems, Foster City, CA). Primers for mouse *Dnase2a* were acquired ready to use from Applied Biosystems, Foster City, CA.

Primers for mouse *Interferon*-β were as follows: *IFN*-β/Fw, 5′-CCACCACAGCCCTCTCCATCAACTAT-3′, and *IFN*-β/Rv, 5′-CAAGTGGAGAGCAGTTGAGGACATC-3′. Primers for mouse *Klf1* were as follows: *mKlf1*/Fw, 5′-AGAAGAGAGAGAGGAGGC-3′, and *mKlf1*/Rv, 5′-AGTGCCGGGAGACTCGGAA-3′. Primers for mouse β-*globin* were as follows: *m*β-*globin*/Fw, 5′-ATGGCCTGAATCACTTGGAC-3′, and *m*β-*globin*/Rv, 5′-ACGATCATATTGCCCAGGAG-3′. Primers for mouse *F4/80* and *GAPDH* were as follows: *F4/80*/Fw, 5′-AAGGAGGACTTCTCCAAGCCTATT-3′, and *F4/80*/Rv, 5′-GAAGTCTGAGAGGCCTATCTGTGTC-3′; *GAPDH*/Fw, 5′-GAGACCCCACTAACATCAAATGG-3′, and *GAPDH*/Rv, 5′-CTTTTGGCTCCACCCTTCAA-3′.

The reactions were performed on three different samples in triplicate, using standard protocols. Samples were normalized with respect to 18S rRNA levels. The analysis of RT-qPCR data was done using the ΔΔ*CT* method (22).

DNase II-alpha enzymatic activity assay. Cell extract from E14.5 *Klf1*$^{+/+}$, *Klf1*$^{+/-}$, and *Klf1*$^{-/-}$ fetal liver was assayed for DNase activity, as described by Kawane et al. (16). The fetal livers were homogenized in lysis buffer (10 mM Tris-HCl [pH 7.5], 1 M NaCl, and 1 mM phenylmethylsulfonyl fluoride [PMSF]). After removing the cells by centrifugation, the supernatant was dialyzed against 50 mM citrate buffer (pH 5.0) containing 1 mM EDTA, and the acid DNase activity was measured, using supercoiled pBS KS plasmid as a substrate. In brief, plasmid DNA (1.5 μg) was mixed with the sample in 100 μl of the reaction mixture (10 mM Tris-HCl [pH 5.7] containing 10 mM EDTA). After incubation at 37°C for 1 h, the mixture was treated with phenol-chloroform, and the DNA was recovered by ethanol precipitation. The DNase II activity was monitored at three different dilutions (1.0, 2.0, and 3.0 μg of proteins), or alternatively a fixed amount (2.0 μg) of protein was assayed at different times of incubation (1 h, 2 h, and 3 h). The integrity of the plasmid DNA was then monitored by electrophoresis on a 0.8% agarose gel.

Histochemical analysis. Livers obtained from E14.5 *Klf1*-null, heterozygous, and wild-type mice were frozen at −80°C and sectioned at 20 μm in a cryostat. The sections collected on gelatin-coated glass slides were fixed in ice-cold acetone for 1 to 2 min and rehydrated in phosphate-buffered saline (PBS). To reduce nonspecific staining, the sections were incubated with 5% normal goat serum in Tris-buffered saline (TBS) for 30 min at room temperature. Samples were then overlaid with rat anti-mouse F4/80 (MCA497R; AbD Serotec, Oxford, United Kingdom) monoclonal antibody (1:50) for 60 min in a humid chamber. Then, slides were rinsed three times and incubated for 30 min with Texas Red-conjugated goat anti-rat IgG (1:200; Vector Laboratories, Burlingame, CA). The sections were rinsed in PBS, mounted in a fluorescent mounting medium, and then examined by fluorescence microscope (Olympus BX-41). Control immunostaining was carried out by the same procedure, except for the utilization of dilution buffer instead of the primary antibody; completely negative results were observed. Cell counts were obtained from pooled livers. Three sections per sample were analyzed, and 5 to 10 fields on the same slide were counted at ×200 magnification.

Double staining. Fetal livers obtained from E13.5 *Klf1*-null and wild-type mice were disrupted by repeated pipetting in PBS. Then, 10 μl of cell suspension was applied on poly-L-lysine-coated slides and fixed in ice-cold acetone for 4 min.

Samples were stained with anti-F4/80 antibody as described above. Successively, cells were washed in PBS plus 0.2% Triton X-100 and then incubated for 1 h with rabbit anti-Klf1 antibody (ab38245, 1:200; Abcam). After washes, samples were overlaid with Alexa Fluor 488-conjugated goat anti-rabbit IgG (Molecular Probes, 1:400) and then stained with Hoechst 33342 dye. Negative controls were performed on the samples with nonimmune serum instead of the primary antibody and then with the appropriate secondary antibody.

Cell culture. Cos-1 cells and Raw 264.7 cells were cultured at 37°C and 5% CO_2 in DMEM (Biochrom AG, Berlin, Germany) supplemented with 10% fetal calf serum and 1% penicillin and streptomycin solution (Gibco-BRL Life Technologies).

Electrophoresis mobility shift analysis (EMSA). A truncated Klf1 protein obtained in a prokaryotic system using Gateway cell technology (Invitrogen) was cloned in plasmid pDEST 17. The 481-amino-acid-long truncated protein containing the three zinc finger binding domains was purified by standard techniques.

EMSA was carried out as previously described (10) with minor modifications: protein was incubated for 20 min at 25°C with 10 fmol/30,000 cpm of a T4 kinase/[γ-^{32}P]ATP-labeled double-strand probe. Reactions were run in 5% acrylamide gels (50/1 cross-linking) in 50 mM Tris-borate buffer at 10 V/cm, dried, and detected by overnight (o/n) autoradiography at −80°C. The sequences of the sense strand of the oligonucleotide probes used in the band shift assay were as follows: β-*globin* proximal CACCC, 5′-CCTGTGGAGCCACACCCTAGGGTTGGCCAAT-3′; *Dnase2a* proximal CACCC, 5′-AGGACGGGGCGGGGAGGACA-3′; *Dnase2a* distal CACCC, 5′-TGCCCAAGGGAGAGGCGTGTC-3′; *Aγ-globin Stage Selector Element* (*SSE*), 5′-GAGGCCAGGGGCCGGCGGCTGGCTAGGGATGA-3′. Quantitative analysis of the shifted bands was carried out on the Storm 840 PhosphorImager (Amersham Biosciences, Amersham, United Kingdom).

Plasmid construction. A 366-bp genomic DNA fragment from the murine *Dnase2a* promoter (−300 to +66 relative to the transcription start site) obtained by PCR with the 5′ HindIII linker primer (5′-CTAAGCTTCATACATGTAGGCAAGACCA-3′) and the 3′ PstI linker primer (5′-CCACTGCAGACGAGATTCAGATGAACTTC-3′) was cloned into the HindIII/PstI site of pMG3 luciferase reporter vector (pDN-α). *Klf1* expression plasmid was prepared by subcloning *Klf1* cDNA driven by the cytomegalovirus (CMV) promoter into the EcoRI site of the pcDNAI vector (Invitrogen). Klf1 binding sites have been mutagenized by standard techniques using the following pairs of oligonucleotides: *Klf1*-prox mut Fw, 5′-AGAAGCGTGAGGACGTTGCGGGGAGGACATTG-3′; *Klf1*-prox mut Rev, 5′-CAATGTCCTCCCCGCAACGTCCTCACGCTTCT-3′.

As a control for transfection efficiency, a plasmid based on the firefly luciferase gene driven by a combination of the HS2 enhancer of the locus control region (LCR) and a NcoI/AccI 450-bp fragment of the β-*globin* promoter (HS2βLuc) was used.

Transactivation assay. Transient transfection of Raw 264.7 cells was performed as follows: aliquots of 1.5×10^6 cells were transfected (in triplicate) in a 30-mm petri dish with 4 μl of DMRIE-C reagent (Invitrogen) per 3 μg of the murine *Dnase2a* promoter reporter vector and 1 μg of KLF1 expression plasmid, grown overnight in serum-free medium, and incubated for 40 more hours in complete medium. Cell extracts were assayed for luciferase activity by the dual reporter assay system (Promega) on a Lumat LB9501 luminometer machine (Berthold and Wallac). All values were normalized for efficiency of transfection by measuring identical amount of protein extracts and by correcting for the activity of a *Renilla*-based expression vector, pRL-TK (Promega), included in an equal amount (1 μg) in each transfection.

Isolation of macrophage. For magnetically activated cell sorting, fetal liver cells from E14.5 wild-type mice and from E14.5 *Klf1*$^{-/-}$ and *Klf1*$^{+/+}$ littermates were collected, homogenized, and resuspended in Macs buffer (PBS, 0.5% bovine serum albumin [BSA], 2 mM EDTA) at a concentration of 1×10^9 cells/ml. To remove the remaining aggregates, the cell suspension was passed through a 30-μm nylon mesh (Pre-Separation filters; Miltenyi Biotec). To isolate the macrophages, cells were first labeled with primary rat anti-mouse F4/80 IgG antibody (MCA497R; AbD Serotec) at the recommended dilutions. Subsequently, the cells were magnetically labeled with goat anti-rat IgG microbeads (130-048-502; Miltenyi Biotec) and the labeled cells were separated, as described by the manufacturer, onto an MS column (Miltenyi Biotec) placed in the magnetic field of a MiniMacs separator (Miltenyi Biotec).

For short-term cell culture, macrophages were also isolated as described by Rhodes et al. (37), with minor modifications. Cells were incubated at 37°C for 90 min before harvesting.

Flow cytometry analysis. F4/80-PE mouse antibody was purchased from BioLegend (San Diego, CA). The flow analysis was performed in a Facs Canto I analyzer (BD, San Jose, CA). Results were analyzed by FlowJo software (Treestar, Ashland, OR).

Construction of shRNA expression vectors and infection. A set of 5 m*Klf1*-specific lentiviral short hairpin RNA (shRNA) constructs in the pLKO.1 vector were obtained from Open Biosystem (Thermo Fisher Scientific Inc., Waltham, MA). The most active shRNA (catalog number TRCN0000071545), containing the sequence CCGGTGAGACTGTCTTACCCTCCATCTCGAGATGGAGGGTAAGACAGTCTCATTTTTG, was used for the experiments of *Klf1* knockdown in primary central macrophages isolated from E13.5 murine fetal livers. Macrophages were infected at a high multiplicity of infection, and RNA was harvested for analysis at 24, 48, and 72 h postinfection. The empty vector pLKO.1 and a *Myb* lentiviral shRNA construct in the pLKO.1 vector (Open Biosystem, Thermo Fisher Scientific Inc., Waltham, MA) were used as a negative control and a KLF1 off-target control, respectively. Lentiviral preparation and transduction of cells were carried out as described previously (26).

ChIP assay. Chromatin immunoprecipitation (ChIP) assays were performed using a kit from Upstate (Temecula, CA). F4/80-positive macrophage cells isolated from E14.5 wild-type fetal mouse liver were used at a concentration of 3×10^5 cells. After formaldehyde fixation (1%), chromatin was fragmented to sizes ranging between 300 and 1,000 bp by sonication, DNA was precleared with protein A conjugated to agarose beads containing salmon sperm DNA, and rabbit polyclonal to Eklf/Klf1 (ab56011; Abcam) primary antibody (4 mg/ml) was added. The anti-Klf1 antibody was tested in Western blotting using fetal liver protein extracts to recognize the target protein at the right size. As a positive control for antibody specificity, a ChIP assay for the mouse β-major CACCC box was carried out using total fetal liver cells (41). Control samples were incubated with protein A beads either without antibody or with a nonspecific antibody [anti-LIFR(C19); Santa Cruz Biotechnology]. Following elution and extraction, immunoprecipitated DNA was analyzed by quantitative real-time PCR (qPCR) using SYBR green (Invitrogen catalog number 11744-500). Primers were designed to amplify a 280-bp DNA fragment centered on the *Klf1* consensus sequence in the m*Dnase2a* promoter region (Prom*Dnase2a*/Fw, 5′-CAAACATACATGTAGGCAAG-3′; Prom*Dnase2a*/Rv, 5′-GGCTTCCTATGAAGTTGTCC-3′). As a negative control, a region around 1 kb upstream and 1 kb downstream from the *Dnase2a* transcription start site (1Kb3′/Fw, 5′-TCCCTCCCGTTCACTCAGTTT-3′; 1Kb3′/Rv, 5′-GACTGGTTCCTCAGAGGAGTTTGA-3′; 1Kb5′/Fw, 5′-GGGACTGGAGAATGGTAAGTTATAGG-3′; 1Kb5′/Rv, 5′-CCTTCCCTCCTGCTTTTGTTT-3′) was examined. A 190-bp DNA fragment in the *MyoD* gene was used as an internal control (*MyoD*1+, 5′-TAACCTTCCACTCCCCTCACAGA-3′; *MyoD*1−, 5′-TGTTCTGTGTCGCTTAGGGATGC-3′).

The analysis was performed on three independent chromatin preparations from macrophage isolated cells. Each sample was analyzed in triplicate to calculate the arithmetic mean (average) and the standard deviation (SD) and *P* value were computed using Student's *t* test.

RESULTS

Mouse *Dnase2a* is downregulated in *Klf1* KO fetal liver. In *Klf1* KO mice, definitive fetal liver erythropoiesis is disrupted, leading to embryonic lethality. Fetal liver erythropoiesis takes place in erythroblastic islands consisting of a central macrophage surrounded by developing erythroblasts. The central macrophage of erythroblastic islands has been suggested to play a critical role in regulating key processes, such as erythroid differentiation and apoptosis through cell/cell interactions, in concert with stimulatory and inhibitory cytokines (24). Furthermore, it has been demonstrated that engulfment and digestion of extruded nuclei by the central macrophage are vital for definitive erythropoiesis in the fetal liver (16, 24). Here, we show that murine *Dnase2a* expression level in fetal liver cells is strongly affected by Klf1 deficiency.

To verify whether the mouse *Dnase2a* is Klf1 dependent, we first examined the expression level of *Dnase2a* in fetal liver cells from E14.5 *Klf1*-null mice compared to that from wt littermates. Semiquantitative RT-PCR showed a significant decrease in *Dnase2a* gene expression in the *Klf1*-null fetal liver cells compared to that in cells with the wt genotype (Fig. 1A). Northern blot analysis (Fig. 1B) performed on wt and *Klf1*-null

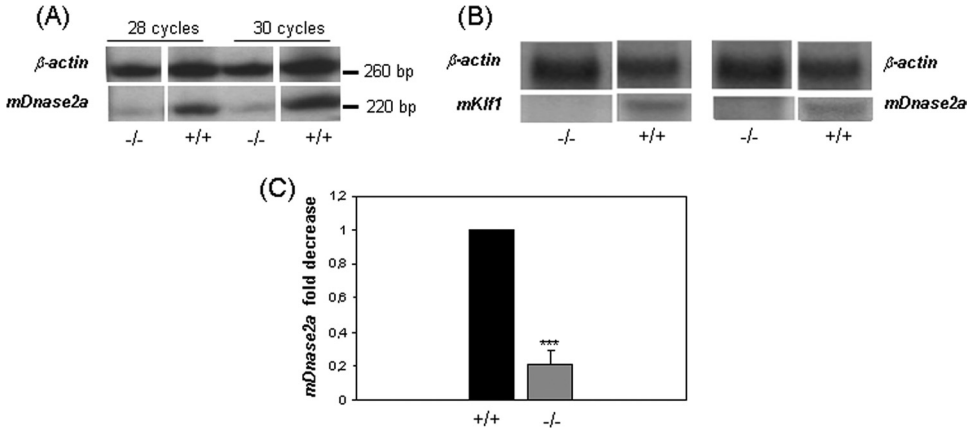

FIG. 1. m*Dnase2a* gene expression analysis in E14.5 *Klf1* wild-type and mutant mice fetal liver. (A) Semiquantitative radioactive time course PCR assay of *Dnase2a* cDNA from E14.5 fetal liver wild-type (+/+) and KO (−/−) *Klf1* embryos. The *mDnase2a* and the β-*actin* reverse primers were end-labeled with [γ-^{32}P]ATP. The 220-bp *mDnase2a* and the 260-bp β-*actin* PCR fragments analyzed at 28 and 30 PCR cycles are shown. (B) Northern hybridization assay of E14.5 wild-type (+/+) and KO (−/−) fetal liver RNA using *mKlf1*, *mDnase2a*, or β-*actin* cDNAs as probes. (C) Relative expression levels of m*Dnase2a* in E14.5 *Klf1*-null (−/−) fetal livers compared with those of the wild-type (+/+) littermates. Levels were quantified by RT-qPCR, and results are expressed as the value relative to the 18S rRNA. ***, $P < 0.001$ according to a *t* test.

E14.5 fetal liver RNA using murine *Klf1* and *Dnase2a* cDNA as probes revealed the absence, as expected, of *Klf1* mRNA and only trace amounts of *Dnase2a* mRNA with respect to the β-*actin* used as a control. Further support for *Dnase2a* dependency on Klf1 was provided by RT-qPCR analysis performed on wt and *Klf1*-null E14.5 fetal liver mRNAs. The expression level of *Dnase2a* mRNA was dramatically reduced (Fig. 1C) in the *Klf1*-null fetal liver compared to that in wt littermates (SD, 0.11; *P*, 0.00014). No significant difference between the wt and the heterozygous littermates was detected.

We next assayed extracts from E14.5 wt, heterozygous, and *Klf1*-null fetal liver cells for DNase II-alpha enzymatic activity. We tested both time course incubation (1-, 2-, and 3-h incubation times; 2 μg of protein) and increasing the amount of protein (1, 2, and 3 μg of protein; 1-h incubation time) on the same cell extract sample as described previously (16). The acid DNase activity was measured by monitoring the input-plasmid DNA integrity. Cell extracts from wt or heterozygous *Klf1* KO fetal liver showed substantial DNase II activity at pH 5.7, resulting in the loss of supercoiled DNA, whereas supercoiled DNA persisted under these conditions in the extracts from *Klf1*-null fetal liver. The enzymatic activity in *Klf1*-null fetal liver cells was strongly reduced in both assays (Fig. 2A and 2B). In contrast, the DNase II-like activity determined at neutral pH in the presence of Ca^{2+} and Mg^{2+} was normal in the extract from *Klf1*-null fetal liver.

Together, these results demonstrate that the *Dnase2a* gene is markedly downregulated in *Klf1*-null fetal liver cells, suggesting that it might also be an Klf1 target gene.

Reduced number and altered morphology of fetal liver macrophages in *Klf1* KO embryos. To analyze fetal liver cells for the presence and function of macrophages, E14.5 mouse liver sections were immunostained with the macrophage-specific marker F4/80. We observed an altered morphology in *Klf1*$^{-/-}$ fetal liver macrophages, in that they were generally round and small and did not show the extensive cytoplasmic projections of normal macrophages (Fig. 3A). Moreover, the number of F4/80^{+} macrophage cells was significantly reduced ($P = 8 \times 10^{-4}$) in the livers of E14.5 *Klf1*-null mice compared to that of their wt and heterozygous littermates (Fig. 3B). The average macrophage number in *Klf1*-null fetal liver sections was 5.7 ± 2.6 per field, compared to 9.7 ± 2.5 per field in the heterozygous and 9.25 ± 1.5 per field in the wt littermates.

IFN-β gene is dysregulated in *Klf1* KO fetal liver. *Interferon*-β mRNA was assayed in the fetal liver of wt and *Klf1*-null E14.5 mice by RT-qPCR analysis. Results showed an increased expression of IFN-β in the *Klf1*-null fetal liver cells (Fig. 3C) ($P < 10^{-4}$).

Klf1 is expressed in fetal liver macrophages. E14.5 fetal liver macrophage cells were isolated by short-term cell culture methods and MACS cell sorting. Cells isolated by short-term culture were all adherent, and more than 95% were F4/80 positive by immunostaining. Figure 4A shows the dot plot of a flow cytometric analysis of isolated fetal liver macrophages. RNA from isolated macrophage cells was analyzed by RT-qPCR to evaluate *Klf1* expression in E14.5 wt (+/+), heterozygous (+/−), and *Klf1*-null (−/−) littermates (Fig. 4B). RT-qPCR assay was also performed on macrophage cells from E14.5 wt mice to assess the expression level of a typical erythroid gene, such as β-*globin*. As shown in Fig. 4C, only trace amounts of β-*globin* expression were detected compared to the erythroid population of the same fetal liver. The isolated macrophages are positive for F4/80, while the erythroid population of the same fetal liver is negative, as assayed by RT-qPCR.

To confirm the presence of Klf1 in fetal liver macrophages, E13.5 wt mouse fetal liver cells were double stained for Klf1 and F4/80 antibody. Figure 4D shows in a single field both positive and negative cells for Klf1 and/or F4/80 (representing the positive and negative controls, respectively). All cells in the field are Hoechst positive (Fig. 4D, panel 1). A great fraction of the cells is Klf1 positive (see left arrow, Fig. 4D, panel 2); most of them are erythroid cells, while others are macrophages (right arrow, Fig. 4D, panel 2), as indicated by the

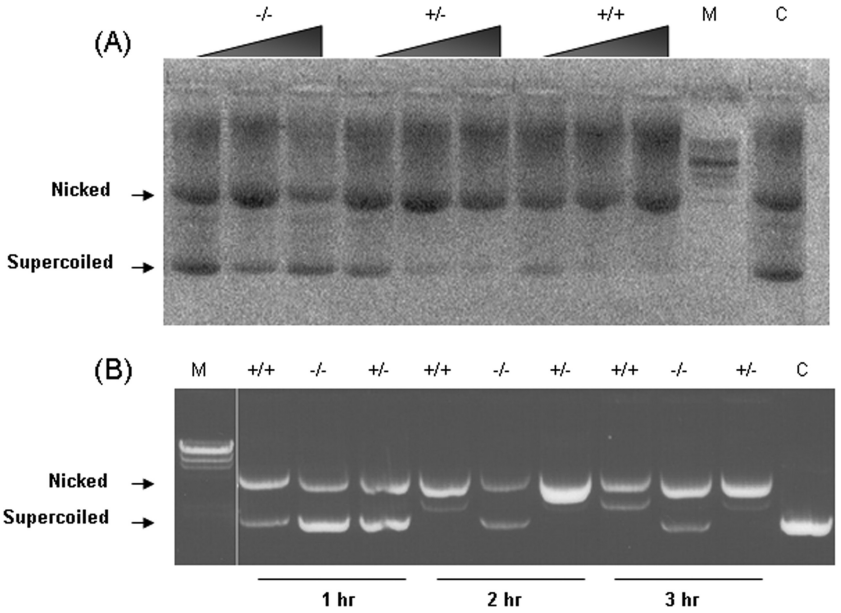

FIG. 2. Assay of DNase II-alpha enzymatic activity. Cell extracts were prepared from E14.5 fetal livers of wild-type (+/+), heterozygous (+/−), and *Klf1*-null (−/−) littermates. DNase II activity at pH 5.7 was determined by evaluation of the supercoiled plasmid DNA integrity monitored by agarose gel electrophoresis. (A) The extracts were assayed at three different dilutions of protein (1.0, 2.0, and 3.0 μg of protein) following 1 h of incubation. (B) Cell extracts with a fixed amount of protein (2.0 μg) were also assayed at three different times of incubation (1.0, 2.0, and 3.0 h). M, molecular size marker DNA; C, input plasmid.

staining for F4/80 (Fig. 4D, panel 3). We quantified the relative percentages of the different cell types. More than 95% of the cells were Klf1 positive, 8% were F4/80 positive, and 7.6% were positive for both F4/80 and Klf1. In *Klf1*-null fetal liver, no positive Klf1 cells were detected. In summary, the results show that Klf1 is expressed and confined to the nucleus in fetal liver cells, including macrophages, as identified by F4/80 immunoreactivity.

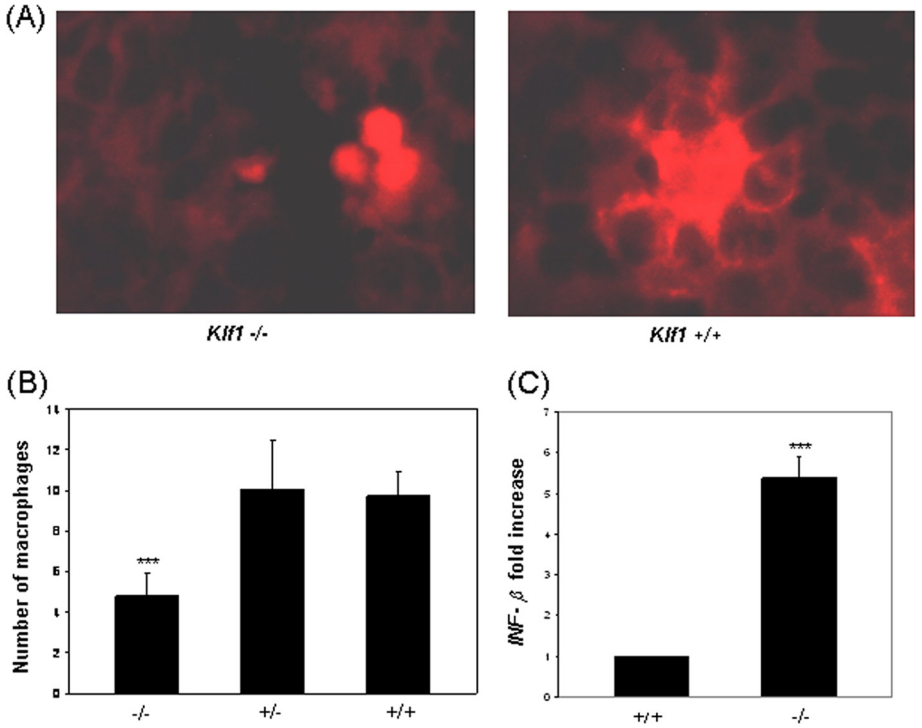

FIG. 3. Histological assay on E14.5 $Klf1^{-/-}$ versus $Klf1^{+/+}$ fetal liver sections. (A) Erythroblastic island central macrophage stained with F4/80 antibody. (B) The diagram shows the number of macrophages/field in E14.5 $Klf1^{-/-}$, $Klf1^{+/-}$, and $Klf1^{+/+}$ fetal liver sections. (C) *IFN*-β gene expression in E14.5 *Klf1*-null fetal liver. The histogram shows *IFN*-β mRNA in E14.5 $Klf1^{-/-}$ versus $Klf1^{+/+}$ fetal livers quantified by RT-qPCR. Results are expressed as the value relative to 18S rRNA. ***, $P < 0.001$ according to a *t* test.

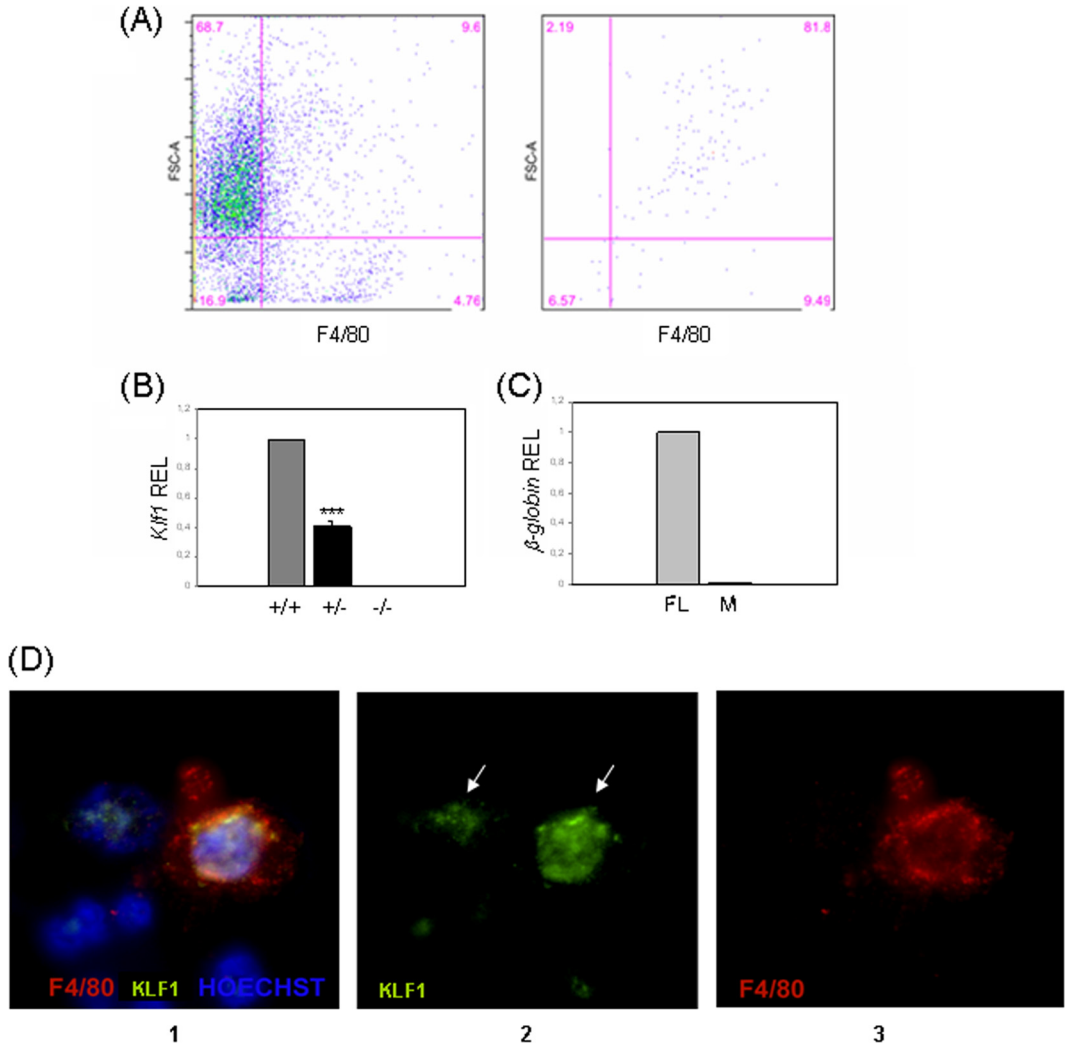

FIG. 4. Expression of *Klf1* gene in F4/80+ macrophage cells. (A) Flow cytometry of fetal liver cells (left) and isolated macrophage cells (right) from E14.5 wild-type mice. Cells were labeled with F4/80-PE antibody. Values shown are percentage of each population among total cells. (B) Relative expression levels of *Klf1* in E14.5 *Klf1*-null (−/−) fetal liver macrophage cells compared with those in the wild-type (+/+) and the heterozygous (+/−) littermates. Levels were quantified by RT-qPCR, and results are expressed as the value relative to the 18S rRNA. (C) E14.5 β-*globin* cDNA obtained from total fetal liver and sorted macrophage cells of wild-type mice was assayed by RT-qPCR. Relative expression levels are expressed as the value relative to that of the 18S rRNA. (D) Double staining of fetal liver cell suspension obtained from E13.5 wt mice. Slides were overlaid with Alexa Fluor 488 conjugated goat anti-rabbit IgG and then stained with Hoechst 33342 dye (panel 1). The same slides were stained with anti-Eklf/Klf1 antibody (panel 2) and anti-F4/80 antibody (panel 3). Arrows in panel 2 indicate some Klf1-positive cells.

DNase II-alpha is upregulated in fetal liver macrophages. We have also analyzed the expression level of *Dnase2a* in freshly isolated primary fetal liver macrophages. Fetal liver macrophages from E14.5 embryos were isolated by short-term culture, and the RNA was analyzed by RT-qPCR and compared to total fetal liver RNA. Three separate experiments were carried out. Expression analysis showed that *Dnase2a* is enriched 9-fold in primary fetal liver macrophages compared with the total fetal liver cells (9.35-fold increase; SD, 1.36; P, $<10^{-3}$).

Klf1 binds and activates *Dnase2a* promoter. To gain insight into the molecular mechanism by which Klf1 may regulate mouse *Dnase2a* expression, we examined the mouse *Dnase2a* promoter. Several GC-rich sequences are present in the murine *Dnase2a* promoter, including two typical Klf1 consensus binding sites, which could possibly confer Klf1 responsiveness (Fig. 5A). A GATA-1 consensus binding site is also present in close proximity to the Klf1 sites. A purified 481-amino-acid-long truncated Klf1 protein containing the full Klf1 binding domain was used to perform EMSA. Only the proximal CACCC motif (Fig. 5B), located from position −63 to position −70 relative to the transcription start site, showed Klf1 binding, whereas the distal one, located from position −125 to position −132 relative to the transcription start site, did not (Fig. 5B) and was therefore not investigated further. An EMSA competition assay showed the specificity of Klf1 binding at the murine *Dnase2a* promoter, as it is competed out by cold oligonucleotides containing the proximal CACCC box of the β-*globin* gene promoter and by itself. The affinity of the *Dnase2a* promoter for Klf1 is lower than that of the β-*globin*

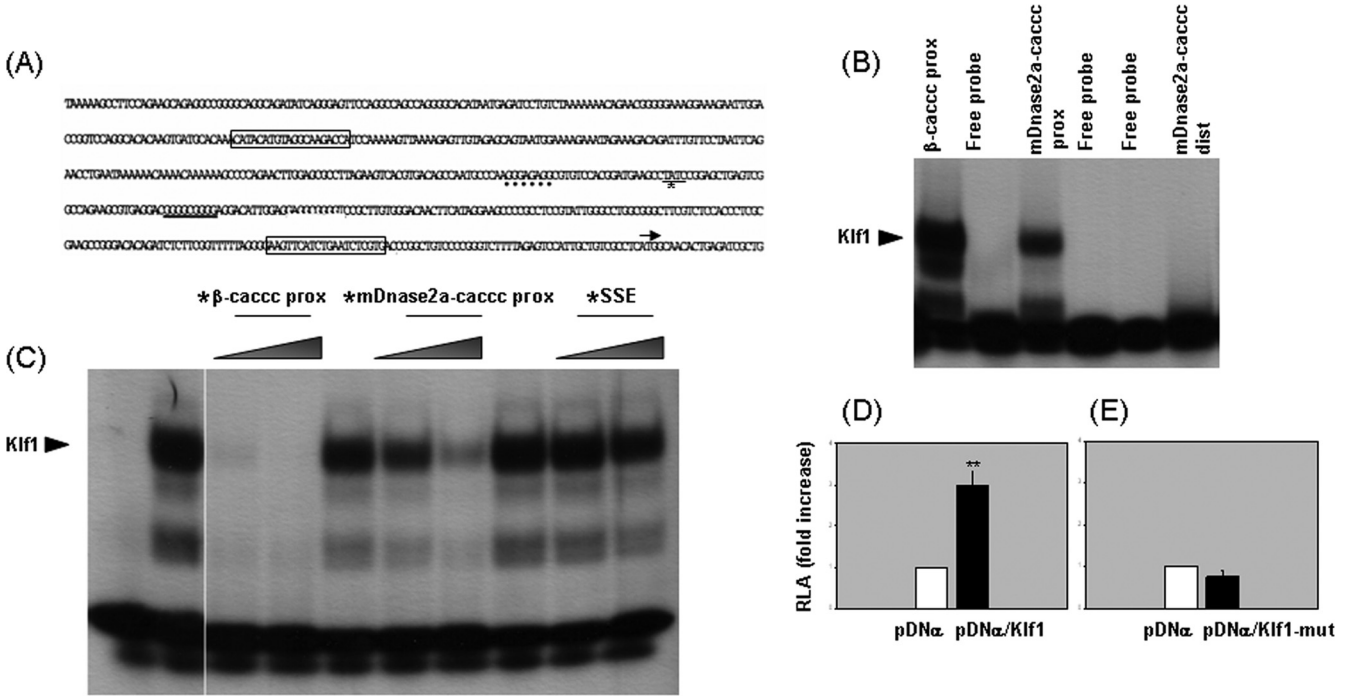

FIG. 5. Klf1 binds and activates *Dnase2a* promoter. (A) Genomic DNA sequence from mouse *Dnase2a* gene promoter. The proximal Klf1 binding site is underlined; the distal putative site is indicated by a dotted line. A GATA1 motif is indicated by an asterisk. The 5′ and 3′ oligonucleotides used to obtain the promoter region used for transfection assay are boxed. The transcription start site is indicated by an arrow. (B) Band shift assay: complexes formed by Klf1-purified truncated protein (indicated by an arrow) with the proximal β-*globin*-CACCC and with the proximal (prox) and distal (dist) *Dnase2*-CACCC promoter probes. (C) Band shift assay: competition of the *Dnase2a*-Klf1 complex (arrow) with the proximal β-CACCC, the *Dnase2a*, and the stage selector element (*SSE*) promoter probes. The cold probes used are indicated on the top of the gel, marked with an asterisk. The gradient-filled triangles represent increasing amounts of the cold competitor. (D and E) Klf1 transactivation assay of the m*Dnase2a* promoter in Raw 264.7 cells. (D) The black and white histograms represent the relative luciferase activities (RLA) expressed as percentages of the reporter (HS2βL) plasmid activity, respectively, observed for cells transfected with the DNase II-alpha expression plasmid (pDn-α/Klf1) and the mock plasmid alone (pDn-α). **, $P < 0.01$ according to a *t* test. (E) RLA observed with the pDn-α/Klf1 plasmid mutagenized in the proximal Klf1-binding site of the *Dnase2a* promoter (pDn-α/Klf1-mut).

gene promoter; nevertheless the binding is not competed out by an unrelated promoter sequence of the *Aγ globin* gene *Stage Selector Element* (SSE), indicating the specificity of the binding (Fig. 5C).

We carried out a transactivation assay in RAW 264.7 cells (mouse leukemic monocyte/macrophage cell line) using a dual reporter luciferase assay. Transactivation experiments were performed using the wt and the proximal CACCC-mutated *Dnase2a* promoter. The mutated proximal CACCC motif does not bind Klf1 *in vitro*. Three independent sets of experiments were carried out in triplicate. We obtained a 3× transactivation of murine *Dnase2a* promoter by Klf1 (SD, 3.3; *P*, 5.6×10^{-5}) (Fig. 5D). Klf1 transactivation was abolished by mutation of the proximal CACCC (Fig. 5E). These data show the ability of Klf1 to bind the CACCC element of the murine *Dnase2a* in gel shift assays and to transactivate the *Dnase2a* promoter in transactivation assay, supporting the direct activation of the *Dnase2a* through the typical CACCC site within the proximal promoter.

Klf1 correlates with and affects *Dnase2a* expression in primary fetal liver macrophages. It has been shown that *Klf1* is not detectable in fetal liver macrophages after several days of culture (11). Therefore, we analyzed the expression levels of *Klf1* and *Dnase2a* in primary fetal liver macrophages over time to establish the optimal temporal window to carry out shRNA-mediated gene silencing assays (see below). Fetal liver macrophages from E13.5 wt mice were isolated by short-term culture, and the RNA was analyzed by RT-qPCR from cells harvested at different time points (24, 37, 48, and 72 h after separation). Three separate experiments were carried out. The analysis revealed that the expression levels of *Klf1* (Fig. 6A) and *Dnase2a* (Fig. 6B) decreased at 24 h after isolation, were highly reduced at 36 h and 48 h after isolation, and were not detectable by 72 h. In contrast, no significant variation was observed in several unrelated genes examined, such as *GAPDH* and β-*actin*, among others. The observed short half-life of *Klf1* and *Dnase2a* in culture is most likely related to the absence of the erythroblastic island niche.

To demonstrate the dependence of the *Dnase2a* expression upon *Klf1*, we used viral transfer technology to silence the gene expression of *Klf1* in primary fetal liver macrophages. The short half-life of *Klf1* (see above) hampered the possibility of carrying out a stable gene expression knockdown assay. *Klf1* was knocked down in primary fetal liver macrophages using a transient shRNA expression assay specifically targeting *Klf1*. The silencing efficiency of the shRNA-based lentiviral vectors was first assessed in pools of MEL cells, and the most active shRNA vector was used for the experiments of *Klf1* gene ex-

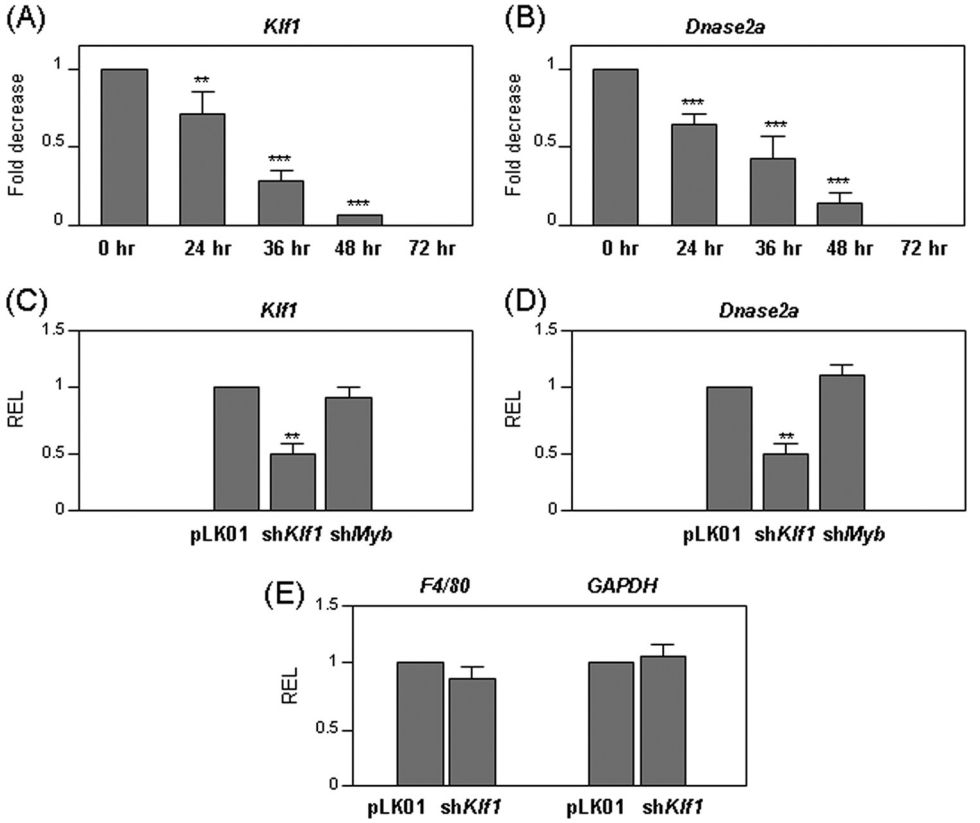

FIG. 6. Expression levels of *Dnase2a* and *Klf1* in primary murine fetal liver macrophage cells after transduction *with mKLF1*-shRNA vector. Total RNA was prepared at several time points from E14.5 and E13.5 wild-type mice fetal liver macrophage cells isolated by a short-term culture method and analyzed by RT-qPCR. (A) Histogram represents the expression level of *Klf1* analyzed at time zero and 24, 36, and 48 h after isolation. ***, $P < 0.001$ according to a *t* test. (B) Histogram represents the expression level of *Dnase2a* analyzed at time zero and 24, 36, and 48 h after isolation. ***, $P < 0.001$ according to a *t* test. (C and D) Histograms show the relative silencing of *Klf1* and *Dnase2a*, following transduction with *mKlf1*-shRNA-mediated lentiviral vector, compared to the status of an empty vector (pLKO.1) and to that of an KLF1 off-target control (*shot*). Cells were harvested at 24 h after infection. **, $P < 0.01$ according to a *t* test. (E) Histograms show the expression levels of *F4/80* and *GAPDH* following transduction with *mKlf1*-shRNA-mediated lentiviral vector compared to that of the empty vector (pLKO.1).

pression knockdown in primary fetal liver macrophages. Cells were harvested at 24 h after infection, and the RNA was analyzed by RT-qPCR.

Klf1-shRNA assays using primary macrophages transduced with the empty packaged lentiviral vector (pLKO.1) as a control revealed a significant reduction of *Klf1* expression (43%; SD = 1.7; *P*, $>10^{-3}$), which correlates with decreased *Dnase2a* expression (42%; SD = 4; *P*, $>10^{-3}$) (Fig. 6C and D). Moreover, no significant reduction in *Klf1* and *Dnase2a* expression was observed after fetal liver macrophage transduction with a lentiviral vector not specifically targeting Klf1 (off-target shRNA, *shot*) (Fig. 6C and D). In addition, the relative expression level of several *Klf1*-unrelated genes such as *F4/80* and *GAPDH* did not significantly change following transduction with *mKlf1*-shRNA lentiviral vector, compared to that with the empty vector pLKO.1 (Fig. 6E).

We conclude that Klf1 expression affects the extent of *Dnase2a* expression in CMEIs.

***In vivo* occupancy of the mouse *Dnase2a* promoter by Klf1.** To assay the direct association of Klf1 with the proximal mouse *Dnase2a* promoter *in vivo*, ChIP analysis was performed on three independent chromatin preparations from isolated E14.5 fetal liver F4/80$^+$ macrophage cells with a Klf1 antibody. The anti-Klf1 antibody was first tested on Western blots using fetal liver protein extracts to show that it recognizes the Klf1 protein by size. An aliquot of cross-linked input DNA was prepared and analyzed as a reference for ChIP efficiency. Quantitative real-time PCR (qPCR) analysis using primers from the mouse *Dnase2a* promoter region was performed to measure the enrichment of anti-Klf1 immunoprecipitated (IP) chromatin. Primers for the *MyoD1* gene were used as an internal control. As shown in Fig. 7A, the *Dnase2a* promoter region was significantly enriched (approximately 5-fold; *P*, 4.7×10^{-5}; *P*, 3.8×10^{-6}, and *P*, 5×10^{-4}) relative to *MyoD1*, indicating Klf1 occupancy. Each histogram in Fig. 7 represents the average of the data derived from three sets of qPCR analysis from three independent fetal liver macrophage purifications. We also examined two regions within 1 kb 5′ and 3′ to the *Dnase2a* transcription start site. The absence of enrichment relative to the negative controls demonstrates the specificity of the assay (Fig. 7A). As a positive control of Klf1 antibody specificity, qPCR analysis with primers from the mouse β-*globin* promoter region was performed on fetal liver cells to measure the enrichment of anti-Klf1 IP chromatin. A

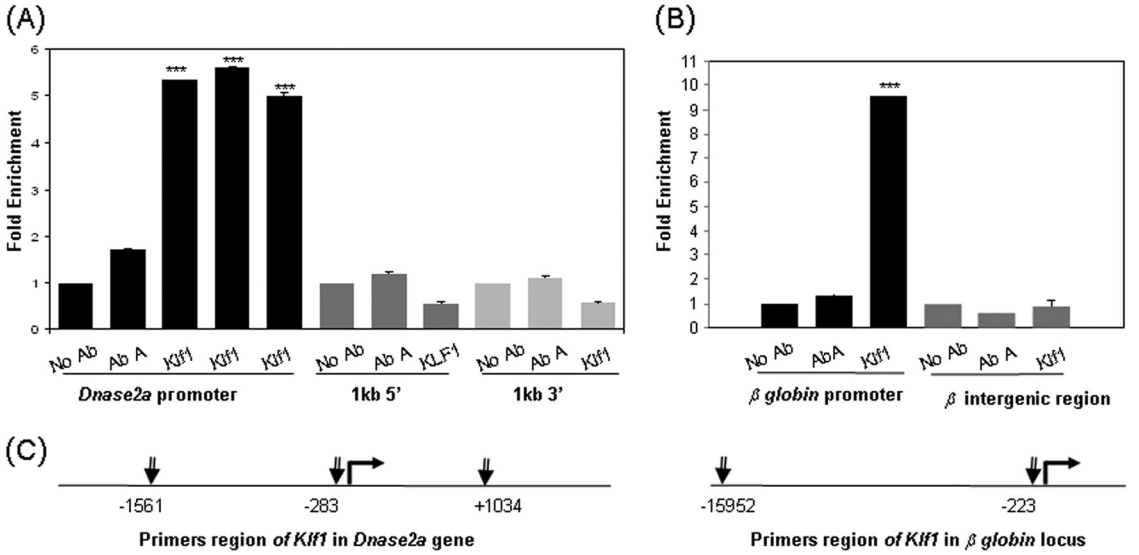

FIG. 7. The m*Dnase2a* promoter is bound by *Klf1 in vivo*. (A) ChIP analysis of the *Dnase2a* promoter and the up- and downstream regions in sorted E14.5 fetal liver macrophage cells from wild-type embryos. Immunoprecipitated (IP) DNA was analyzed by qPCR with several sets of primers from the m*Dnase2a* promoter region (centered on the proximal *Klf1* consensus binding motif), the 5′ and 3′ regions 1 kb upstream and downstream of the gene, and the *MyoD1* gene. (B) ChIP assay of the mouse β-*globin* gene promoter in sorted E14.5 fetal liver macrophage cells from wt embryos. IP DNA was analyzed by qPCR with primers from the mouse β-*globin* gene promoter (centered on the proximal CACCC motif) and from an intergenic region in the mouse β-*globin* locus as a negative control. Histograms represent the relative *Klf1* enrichment compared to those of the DNA sample without antibody (No Ab) and the sample with a nonspecific antibody (Ab A), calculated by the averages of data derived from three independent ChIP assays. Results are expressed as the value relative to the *MyoD1* gene, used as an internal control. ***, $P < 0.001$ according to a *t* test. (C) Schematic diagram showing the location of ChIP primers as downward arrows with respect to the transcription start site across the mouse *Dnase2a* and the mouse β-*globin* gene promoters.

10-fold specific enrichment, compared to the control, was obtained (Fig. 7B). An intergenic region in the mouse β-*globin* locus was also examined as a negative control in the assay (Fig. 7B).

These results show Klf1 occupancy of the relevant region of the mouse *Dnase2a* promoter containing the Klf1 binding site and strongly suggest that *Dnase2a* is a direct Klf1 target gene in fetal liver primary macrophage cells and support the notion that *Klf1* deficiency leads to decreased expression of the *Dnase2a*, contributing to the defective late-stage erythropoiesis in fetal liver erythroblastic islands.

DISCUSSION

Definitive erythropoiesis takes place in erythroblastic islands in mammals. Erythroblastic islands are highly specialized hematopoietic tissue subcompartments that play a critical role in regulating erythropoiesis. Erythroblastic islands contain a central macrophage surrounded by erythroid cells at different stage of maturation. The central macrophage is different from other resident macrophages and can be distinguished by the surface expression of F4/80 antigen and Forssman glycosphingolipid and by the absence of Mac-I antigen (for a review, see the work of Manwani and Bieker [24]). The role of the central macrophage in erythroid maturation involves the engulfment of extruded nuclei from erythroblasts and degradation of the nuclear DNA by DNase II-alpha (27).

In the fetal liver, nuclei expelled from the developing erythroblast rapidly expose phosphatidylserine on their surface and are phagocytosed by the central fetal liver macrophages (17, 48). The mechanisms of erythroblastic island formation, macrophage-erythroid cell interaction, and cytokine expression are not fully understood. Cell-cell interactions seem to be mediated by different proteins, but only a few have been characterized (8, 18, 39, 43).

One of the main established roles of the central macrophage is to phagocytose and degrade DNA contained in erythrocyte nuclei (27). The lack or dysfunction of the central macrophage, as in retinoblastoma-KO mice, results in embryonic lethality, anemia, and abnormal maturation of definitive erythroblasts that fail to enucleate (15, 50). Gene ablation experiments revealed that *Dnase2a* is indispensable for definitive erythropoiesis and is responsible for destroying the nuclear DNA expelled from developing erythroid cells. Lack of DNase II-alpha activity is associated with persistence of nucleated definitive erythrocytes in the fetus. Homozygous *Dnase2a*-null embryos develop normally up to E12, becoming progressively anemic afterwards and dying around E17 (16). The defect in definitive erythropoiesis has been established to be non-cell autonomous because liver cells from *Dnase2a*$^{-/-}$ mice transplanted into wt mice developed into mature enucleated cells (16). The central macrophage with no DNase II-alpha is unable to digest nuclear DNA expelled from the developing erythrocyte. *Dnase2a*$^{-/-}$ mice suffer from severe anemia due to IFN-β production. Accumulation of DNA directly triggers the production of interferon-β by the central macrophage and induces expression of interferon-responsive genes that cause the embryonic lethality (49). IFN-β has a cytotoxic effect on erythroid cells and inhibits erythroid cell growth in a dose-dependent manner (49). Activation of IFN-β is one of the markers of the activa-

tion of innate immunity. Innate immunity is activated in *Dnase2a*$^{-/-}$ mice in a Toll-like receptor (TLR)-independent mechanism (49). The signal molecules linking DNase II-alpha deficiency to IFN-β production remain to be determined, but it has recently been shown that IFN-β production can be stimulated by threonine-phosphatase of Eyes absent 4 (EyA4) in response to undigested DNA (30).

Here we show that *Klf1* is expressed in CMEI and that *Dnase2a* is strongly downregulated in the fetal liver of *Klf1* KO mice. *Dnase2a* downregulation in *Klf1* KO mouse fetal liver macrophages has not been previously reported (6, 14, 28, 36). We have also shown that DNase II enzymatic activity is reduced in *Klf1* null mice, fetal liver macrophages are abnormal, their number is decreased, and IFN-β is activated. In addition, we have shown that the promoter of the murine *Dnase2a* contains a *Klf1* consensus sequence that is bound *in vitro* by Klf1 in EMSA experiments and *in vivo* in ChIP assay. This sequence is responsible for transactivation of the *Dnase2a* promoter by Klf1 in a murine macrophage cell line.

Lentivirus-mediated *Klf1*-shRNA interference showed a significant downregulation of *Klf1* and *Dnase2a* in transduced CMEIs.

These results show that *Dnase2a* is a direct target of Klf1 and that Klf1 regulates the expression of *Dnase2a* in the CMEI. The results further suggest that Klf1 controls the CMEI-specific upregulation of *Dnase2a* necessary to efficiently degrade the nuclear DNA from developing erythrocytes. A lack of Klf1 lowers DNase II-alpha activity, which slows the capacity of the central macrophage to digest DNA, resulting in activation of IFN-β, which would contribute to the impairment of the definitive erythropoiesis.

Trace amounts of mouse β-*globin* expression have been detected in isolated primary fetal liver macrophages. Even though expression of globins in macrophages has been reported before (21), this result could also be explained by the presence of residual erythroid cells. However, the expression of *Klf1* in CMEI has been confirmed here by immunohistochemical analysis.

The decreased number of macrophages in *Klf1* KO fetal liver may represent a secondary effect of DNase II-alpha shortage and is only marginally responsible for the 5-fold DNase II-alpha downregulation observed in *Klf1* KO fetal liver, taking into account the 9-fold upregulation of DNase II-alpha in the CMEI.

Taken together, these data indicate a non-cell-autonomous role of Klf1 in definitive erythropoiesis in addition to its cell-autonomous role. A non-cell-autonomous role of Klf1 has been previously suggested by Perkins et al. (33) to explain the incongruity between the full *Klf1* KO mice and *Klf1* KO/wt chimeras. Lim et al. (20) first showed that *Klf1*-null embryonic stem (ES) cells injected into wt blastocysts were able to undergo erythropoiesis and produce enucleated erythrocytes with an extended life span when a γ-globin transgene was present. Subsequently, Perkins et al. (33) attempted to rescue the *Klf1*$^{-/-}$ phenotype by mating *Klf1*$^{+/-}$ mice with a transgenic line expressing a high level of the γ-*globin* gene (γ+). Surprisingly, *Klf1*-null γ+ expressing mice did not have any survival advantage compared to the *Klf1*-null γ− mouse littermates, even though the globin chain balance was restored.

In one report, the authors mainly employed the *in vitro* culture of primary erythroid progenitors, thus lacking macrophages (6). In another report, an erythroblast immortalized cell line (cell line B1.6) and E14 fetal liver were analyzed, and only those genes that were up- or downregulated in both biological samples were taken into consideration, therefore excluding the genes expressed in macrophages (14). In data obtained by subtractive hybridization, only a few downregulated genes were identified, overlooking most of the genes found to be downregulated by microarray expression profile experiments (36). In addition, microarrays used by the authors were not representative of the full genome and in some cases were enriched for erythroid-specific genes (6, 14, 28, 36).

Enucleated definitive red cells are a feature of mammals. In fish, amphibian, reptiles and birds, definitive erythrocytes are nucleated. The lack of enucleated red cells correlates with the absence of erythroblastic islands in definitive erythropoietic tissue in birds (2) and seems to correlate to the absence of DNase II-alpha in nonmammalian vertebrates. Only in mammals (http://www.ncbi.nlm.nih.gov/gene, http://www.ensembl.org), two members of the DNase II enzyme family have been identified: DNase II-alpha, involved in definitive erythropoiesis, and DNase II-beta, involved in lens cells differentiation. The only other *Dnase2a* present in the public databases (http://www.ncbi.nlm.nih.gov/gene, http://www.ensembl.org) is the single *Dnase2* of *Danio rerio*, in which no Klf1 binding site is present in the proximal promoter region, in agreement with the status of nucleated definitive red cells in fish.

Our observations, along with those previously reported by others, highlight Klf1 as a key factor of definitive erythropoiesis contributing to the regulation of both cell-autonomous and non-cell-autonomous mechanisms. A non-cell-autonomous role of Klf1 in erythropoiesis is strongly suggested by the presence of mature enucleated erythrocytes in *Klf1*-null/*wt* chimeric mice (20, 33). This predicts that in a CMEI conditional *Klf1* KO mouse model, nucleated definitive red cells with normal erythropoiesis would be present. Klf1 may regulate additional genes in fetal liver macrophages. Its full role in the CMEI, and therefore its role in the fetal liver blood island homeostasis, needs further investigation.

In summary, we have shown that Klf1 has a non-cell-autonomous role in definitive erythropoiesis through the regulation of DNase II-alpha activity in the central macrophages of erythroblastic islands. The downregulation of DNase II-alpha activates the production of IFN-β in macrophages, which, via an as-yet-to-be-elucidated mechanism, contributes to the block in erythroid differentiation in *Klf1*-null mice.

ACKNOWLEDGMENTS

We thank Marcella Arras and Federica Piras, Service of Cytofluorimetric Diagnosis and Stem Cell Therapy, Bone Marrow Transplantation Center, R. Binaghi Hospital, Cagliari, Italy.

This work has been partially supported by Regione Autonoma della Sardegna.

REFERENCES

1. **Bieker, J. J.** 2005. Probing the onset and regulation of erythroid cell-specific gene expression. Mt. Sinai J. Med. **72:**333–338.
2. **Campbell, F.** 1967. Fine structure of the bone morrow of the chicken and pigeon. J. Morphol. **123:**405–439.
3. **Ciavatta, D. J., T. M. Ryan, S. C. Farmer, and T. M. Townes.** 1995. Mouse model of human beta zero thalassemia: targeted deletion of the mouse beta maj- and beta min-globin genes in embryonic stem cells. Proc. Natl. Acad. Sci. U. S. A. **92:**9259–9263.

4. **Donze, D., T. M. Townes, and J. J. Bieker.** 1995. Role of erythroid Kruppel-like factor in human gamma- to beta-globin gene switching. J. Biol. Chem. **270:**1955–1959.
5. **Drissen, R., et al.** 2004. The active spatial organization of the beta-globin locus requires the transcription factor EKLF. Genes Dev. **18:**2485–2490.
6. **Drissen, R., et al.** 2005. The erythroid phenotype of EKLF-null mice: defects in hemoglobin metabolism and membrane stability. Mol. Cell. Biol. **25:**5205–5214.
7. **Evans, C. J., and R. J. Aguilera.** 2003. DNase II: genes, enzymes and function. Gene **322:**1–15.
8. **Fabriek, B. O., et al.** 2007. The macrophage CD163 surface glycoprotein is an erythroblast adhesion receptor. Blood **109:**5223–5229.
9. **Feng, W. C., C. M. Southwood, and J. J. Bieker.** 1994. Analyses of beta-thalassemia mutant DNA interactions with erythroid Krüppel-like factor (EKLF), an erythroid cell-specific transcription factor. J. Biol. Chem. **269:**1493–1500.
10. **Fried, M., and D. M. Crothers.** 1981. Equilibria and kinetics of lac repressor-operator interaction by polyacrylamide gel electrophoresis. Nucleic Acids Res. **9:**6505–6525.
11. **Frontelo, P., et al.** 2007. Novel role for EKLF in megakaryocyte lineage commitment. Blood **110:**3871–3880.
12. **Funnell, A. P., et al.** 2007. Erythroid Krüppel-like factor directly activates the basic Krüppel-like factor gene in erythroid cells. Mol. Cell. Biol. **27:**2777–2790.
13. **Goodwin, A. J., J. M. McInerney, M. A. Glander, O. Pomerantz, and C. H. Lowrey.** 2001. In vivo formation of a human beta-globin locus control region core element requires binding sites for multiple factors including GATA-1, NF-E2, erythroid Kruppel-like factor, and Sp1. J. Biol. Chem. **276:**26883–26892.
14. **Hodge, D., et al.** 2006. A global role for EKLF in definitive and primitive erythropoiesis. Blood **107:**3359–3370.
15. **Iavarone, A., et al.** 2004. Retinoblastoma promotes definitive erythropoiesis by repressing Id2 in fetal liver macrophages. Nature **432:**1040–1045.
16. **Kawane, K., et al.** 2001. Requirement of DNase II for definitive erythropoiesis in the mouse fetal liver. Science **292:**1546–1549.
17. **Kunisaki, Y., et al.** 2004. Defective fetal liver erythropoiesis and T lymphopoiesis in mice lacking the phosphatidylserine receptor. Blood **103:**3362–3364.
18. **Lee, G., et al.** 2006. Targeted gene deletion demonstrates that the cell adhesion molecule ICAM-4 is critical for erythroblastic island formation. Blood **108:**2064–2071.
19. **Lee, J. S., H. Ngo, D. Kim, and J. H. Chung.** 2000. Erythroid Kruppel-like factor is recruited to the CACCC box in the beta-globin promoter but not to the CACCC box in the gamma-globin promoter: the role of the neighboring promoter elements. Proc. Natl. Acad. Sci. U. S. A. **97:**2468–2473.
20. **Lim, S. K., J. J. Bieker, C. S. Lin, and F. Costantini.** 1997. A shortened life span of EKLF−/− adult erythrocytes, due to a deficiency of beta-globin chains, is ameliorated by human gamma-globin chains. Blood **90:**1291–1299.
21. **Liu, L., M. Zeng, and J. S. Stamler.** 1999. Hemoglobin induction in mouse macrophages. Proc. Natl. Acad. Sci. U. S. A. **96:**6643–6647.
22. **Livak, K. J., and T. D. Schmittgen.** 2001. Analysis of relative gene expression data using real-time quantitative PCR and the $2^{-\Delta\Delta C}$T method. Methods **25:**402–408.
23. **Luo, Q., et al.** 2004. Activation and repression of interleukin-12 p40 transcription by erythroid Kruppel-like factor in macrophages. J. Biol. Chem. **279:**18451–18456.
24. **Manwani, D., and J. J. Bieker.** 2008. The erythroblastic island. Curr. Top. Dev. Biol. **82:**23–53.
25. **Miller, I. J., and J. J. Bieker.** 1993. A novel, erythroid cell-specific murine transcription factor that binds to the CACCC element and is related to the Krüppel family of nuclear proteins. Mol. Cell. Biol. **13:**2776–2786.
26. **Moffat, J., D. A. Grueneberg, X. Yang, S. Y. Kim, A. M. Kloepfer, G. Hinkle, B. Piqani, T. M. Eisenhaure, B. Luo, J. K. Grenier, A. E. Carpenter, S. Y. Foo, S. A. Stewart, B. R. Stockwell, N. Hacohen, W. C. Hahn, E. S. Lander, D. M. Sabatini, and D. E. Root.** 2006. A lentiviral RNAi library for human and mouse genes applied to an arrayed viral high-content screen. Cell **124:**1283–1298.
27. **Nagata, S.** 2005. DNA degradation in development and programmed cell death. Annu. Rev. Immunol. **23:**853–875.
28. **Nilson, D. G., D. E. Sabatino, D. M. Bodine, and P. G. Gallagher.** 2006. Major erythrocyte membrane protein genes in EKLF-deficient mice. Exp. Hematol. **34:**705–712.
29. **Nuez, B., D. Michalovich, A. Bygrave, R. Ploemacher, and F. Grosveld.** 1995. Defective haematopoiesis in fetal liver resulting from inactivation of the EKLF gene. Nature **375:**316–318.
30. **Okabe, Y., T. Sano, and S. Nagata.** 2009. Regulation of the innate immune response by threonine-phosphatase of Eyes absent. Nature **460:**520–524.
31. **Pearson, R., J. Fleetwood, S. Eaton, M. Crossley, and S. Bao.** 2008. Krüppel-like transcription factors: a functional family. Int. J. Biochem. Cell Biol. **40:**1996–2001.
32. **Perkins, A. C., K. M. Gaensler, and S. H. Orkin.** 1996. Silencing of human fetal globin expression is impaired in the absence of the adult beta-globin gene activator protein EKLF. Proc. Natl. Acad. Sci. U. S. A. **93:**12267–12271.
33. **Perkins, A. C., K. R. Peterson, G. Stamatoyannopoulos, H. E. Witkowska, and S. H. Orkin.** 2000. Fetal expression of a human Agamma globin transgene rescues globin chain imbalance but not hemolysis in EKLF null mouse embryos. Blood **95:**1827–1833.
34. **Perkins, A. C., A. H. Sharpe, and S. H. Orkin.** 1995. Lethal beta-thalassaemia in mice lacking the erythroid CACCC-transcription factor EKLF. Nature **375:**318–322.
35. **Pilon, A. M., et al.** 2008. Failure of terminal erythroid differentiation in EKLF-deficient mice is associated with cell cycle perturbation and reduced expression of E2F2. Mol. Cell. Biol. **28:**7394–7401.
36. **Pilon, A. M., et al.** 2006. Alterations in expression and chromatin configuration of the alpha hemoglobin-stabilizing protein gene in erythroid Kruppel-like factor-deficient mice. Mol. Cell. Biol. **26:**4368–4377.
37. **Rhodes, M. M., P. Kopsombut, M. C. Bondurant, J. O. Price, and M. J. Koury.** 2008. Adherence to macrophages in erythroblastic islands enhances erythroblast proliferation and increases erythrocyte production by a different mechanism than erythropoietin. Blood **111:**1700–1708.
38. **Ristaldi, M. S., et al.** 2001. The role of the -50 region of the human gamma-globin gene in switching. EMBO J. **20:**5242–5249.
39. **Sadahira, Y., T. Yoshino, and Y. Monobe.** 1995. Very late activation antigen 4-vascular cell adhesion molecule 1 interaction is involved in the formation of erythroblastic islands. J. Exp. Med. **181:**411–415.
40. **Schoenfelder, S., et al.** 2010. Preferential associations between co-regulated genes reveal a transcriptional interactome in erythroid cells. Nat. Genet. **42:**53–61.
41. **Shyu, Y. C., et al.** 2006. Chromatin-binding *in vivo* of the erythroid kruppel-like factor, EKLF, in the murine globin loci. Cell Res. **16:**345–355.
42. **Siatecka, M., F. Lohmann, S. Bao, and J. J. Bieker.** 2010. EKLF directly activates the p21WAF1/CIP1 gene by proximal promoter and novel intronic regulatory regions during erythroid differentiation. Mol. Cell. Biol. **30:**2811–2822.
43. **Soni, S., et al.** 2006. Absence of erythroblast macrophage protein (Emp) leads to failure of erythroblast nuclear extrusion. J. Biol. Chem. **281:**20181–20189.
44. **Southwood, C. M., K. M. Downs, and J. J. Bieker.** 1996. Erythroid Krüppel-like factor exhibits an early and sequentially localized pattern of expression during mammalian erythroid ontogeny. Dev. Dyn. **206:**248–259.
45. **Tallack, M. R., J. R. Keys, P. O. Humbert, and A. C. Perkins.** 2009. EKLF/KLF1 controls cell cycle entry via direct regulation of E2f2. J. Biol. Chem. **284:**20966–20974.
46. **Tallack, M. R., J. R. Keys, and A. C. Perkins.** 2007. Erythroid Kruppel-like factor regulates the G1 cyclin dependent kinase inhibitor p18INK4c. J. Mol. Biol. **369:**313–321.
47. **Tallack, M. R., et al.** 2010. A global role for KLF1 in erythropoiesis revealed by ChIP-seq in primary erythroid cells. Genome Res. **20:**1052–1063.
48. **Yoshida, H., et al.** 2005. Phosphatidylserine-dependent engulfment by macrophages of nuclei from erythroid precursor cells. Nature **437:**754–758.
49. **Yoshida, H., Y. Okabe, K. Kawane, H. Fukuyama, and S. Nagata.** 2005. Lethal anemia caused by interferon-beta produced in mouse embryos carrying undigested DNA. Nat. Immunol. **6:**49–56.
50. **Walkley, C. R., V. G. Sankaran, and S. H. Orkin.** 2008. Rb and hematopoiesis: stem cells to anemia. Cell Div. **3:**13.
51. **Wijgerde, M., et al.** 1996. The role of EKLF in human beta-globin gene competition. Genes Dev. **10:**2894–2902.
52. **Zhou, D., K. Liu, C. W. Sun, K. M. Pawlik, and T. M. Townes.** 2010. KLF1 regulates Bcl11A expression and gamma to beta globin gene switching. Nat. Genet. **42:**742–744.